Evaluation on the Steady-state Assumption of the Global Vegetation Carbon from Multi-Decadal Space-borne Observations

Naixin Fan[1,2*], Maurizio Santoro[3], Simon Besnard[4], Oliver Cartus[3], Sujan Koirala[1] and Nuno Carvalhais[1,5*]

[1]Max Planck Institute for Biogeochemistry, Hans Knöll Strasse 10, 07745 Jena, Germany

[2]Technische Universität Dresden, Institute of Photogrammetry and Remote Sensing, Helmholtzstr. 10, 01069, Dresden, Germany

[3]Gamma Remote Sensing, 3073 Gümligen, Switzerland

[4]Laboratory of Geo-Information Science and Remote Sensing, Wageningen University & Research, The Netherlands

[5]Departamento de Ciências e Engenharia do Ambiente, DCEA, Faculdade de Ciências e Tecnologia, FCT, Universidade Nova de Lisboa, 2829-516 Caparica, Portugal

* Corresponding authors: Naixin Fan (nfan@bgc-jena.mpg.de) and Nuno Carvalhais (ncarvalhais@bgc-jena.mpg.de)

Key Points:

- Using global annual above-ground vegetation biomass data from 1992 to 2016, we estimate vegetation carbon turnover times globally in a non-steady state.
- At the grid cell level, the assumption of steady-state in vegetation biomass can cause substantial biases, especially in regions where there are disturbances from anthropogenic activities or natural causes.
- Despite these local differences, we found that the steady-state assumption can be made at large spatial scales (greater than approximately 15º) as the changes in biomass proportional to the total biomass decrease with the increasing spatial scales.

Abstract

Vegetation turnover time ( ) is a central ecosystem property to quantify the global vegetation carbon dynamics. However, our understanding of vegetation dynamics is hampered by the lack of long-term observations of the changes in vegetation biomass. Here we challenge the steady state assumption of by using annual changes in vegetation biomass that derived from remote-sensing observations. We evaluate the changes in magnitude, spatial patterns, and uncertainties in vegetation carbon turnover times from 1992 to 2016. We found that the forest ecosystem is close to a steady state at global scale, contrasting with the larger differences between under steady state and under non-steady state at the grid cell level. The observation that terrestrial ecosystems are not

in a steady state locally is deemed crucial when studying vegetation dynamics and the potential response of biomass to disturbance and climatic changes.

Plain Language Summary

The lack of observations hampers the current understanding of forest vegetation temporal dynamics. In this study, we use long-term global observations of vegetation biomass retrieved from satellite observations to estimate vegetation carbon turnover times. Our results show that the assumption of a steady state is robust at the global scale, but does not hold at the local scale.

1 Introduction

One of the largest uncertainties in Earth system models is in quantifying how the carbon uptake by terrestrial ecosystems will respond to changes in climate (Friedlingstein et al. 2006; Friend et al., 2014). As an emergent ecosystem property that partially determines carbon sequestration capacity, the vegetation biomass turnover times ( ) have been used as a diagnostic metric to quantify the feedback between the carbon cycle and climate (Carvalhais et al., 2014; Thurner et al., 2016). However, there is a large uncertainty in the simulations of vegetation carbon stock as well as across earth system models, indicating different representations of the response of vegetation to future climate change (Friend et al. 2014). Furthermore, our current understanding of and the dynamic of vegetation is limited due to the lack of long-term observations of changes in vegetation. As a result, the estimation of has relied so far on the assumption that the vegetation carbon in an ecosystem will eventually reach a steady state (steady state assumption, hereafter SSA) at which the net change of vegetation biomass becomes zero (C_{veg}=0), or so small compared to the total biomass that becomes negligible. The SSA has been shown to be a useful assumption at a large spatial scale. However, at local scales, an ecosystem is unlikely to maintain a steady state due to the influences from external factors such as disturbances and climate variability (Ge et al., 2019). It is still unknown whether the SSA can hold at local spatial domains and how much the difference it can make to the estimation if one neglects the temporal changes in vegetation carbon.

In this study, we used estimates of annual changes in vegetation carbon derived from a multi-decadal dataset and global estimations of gross primary productivity (GPP) that are driven by meteorological observations (Besnard et al., 2021; Santoro et al., 2022; Tramontana et al. 2016; Jung et al. 2020), for estimating and comparing estimates that are derived from SSA and non-steady-state assumption (hereafter NSSA), respectively, at local, biome and global scales. The validity of SSA was evaluated in different spatial domains to better quantify the effect of spatial scales on the patterns of carbon turnover times.

2 Data and Methods

In this section, we first introduce the datasets we used to estimate including above-ground vegetation biomass, below-ground biomass and gross primary pro-

ductivity. We used a forest canopy cover dataset to examine the relationship between the changes in and tree canopy cover. Then the calculations of using three methods are introduced next with detailed explanations.

2.1 The multi-decadal estimates of AGB dataset

Annual AGB estimates were derived from C-band satellite radar signals between 1992 and 2016 with a pixel size of 25 km (Santoro et al., 2022). The very dense time series of observations by the European Remote Sensing (ERS) WindScatterometer, the MetOp Advanced SCATterometer (ASCAT), and the Envisat Advanced Synthetic Aperture Radar (ASAR) were used to maximize the information content of forest structure in the signal, allowing for AGB estimates of higher accuracy compared to values obtained from a single observation (Santoro et al., 2022). The annual estimation of AGB is obtained by synthesizing all daily observations of the radar backscatter at one location in a pixel ($0.25^{o}\times0.25^{o}$), enabling the inference of a continuous time series of AGB estimation. By adapting the AGB retrieval method in time and space and computing a weighted average of individual AGB estimates, the annual AGB estimates were less impacted by data noise, instantaneous moisture conditions, precipitation, and snow cover (Santoro et al., 2011).

2.2 Estimation of total vegetation carbon stock

The stock of total vegetation biomass consists of AGB and BGB. Therefore, we estimated BGB from the AGB time series by scaling with the root-shoot ratio, Rrs:

$$BGB = AGB \times R_{\mathrm{rs}} \quad (1)$$

In this study, we used a spatially explicit global dataset of root-shoot ratio, which was derived from a machine learning model that is trained on a large number of ground field measurements of forest root biomass as a function of shoot biomass, tree height, age, species, topography, land management, edaphic and climate covariates (Huang et al., 2021).

The total vegetation carbon was obtained by summing the carbon in both AGB and BGB under the assumption that the carbon stock is 47% of the total dry biomass (IPCC, 2006):

$$C_{\mathrm{veg}} = A\mathrm{GB} \ \times (1 + R_{\mathrm{rs}}) * 0.47 \quad (2)$$

2.3 GPP dataset

We used estimations of GPP from the FLUXCOM project in which different machine learning approaches were applied to upscale global energy and carbon fluxes from eddy covariance flux measurements (Tramontana et al., 2016; Jung et al., 2020). In this study, GPP annual estimates driven by meteorological observations and remote sensing observations at the spatial resolution of 0.5^{o} and

the time period from 1992 to 2016 are used as carbon influx into the vegetation carbon pool. The dataset was resampled to the spatial resolution of 0.25° to match the AGB dataset.

2.4 Forest tree canopy cover change

Tree canopy cover (vegetation that is greater than 5 meters in height) was derived from the Advanced Very High Resolution Radiometer (AVHRR) remote-sensing measurements (Song et al., 2018). The version 4 Long Term Data Record (LTDR) was used to generate the data on tree canopy coverage from 1982 to 2016. Daily LTDR surface reflectance data were used to compute the normalized difference vegetation index (NDVI) at each pixel (0.05°×0.05°). Maximum NDVI composition was then used to obtain adjusted annual phenological metrics, which were used as input to supervised regression tree models to generate the annual product of tree canopy coverage.

2.5 Estimation of under steady state

Changing C_{veg} over time is determined by the uptake of carbon and turnover times:

$$\frac{dC_{veg}}{dt} = GPP - \frac{C_{veg}}{\tau} \quad (3)$$

C_{veg} is the vegetation carbon stock. Assuming that the vegetation carbon pool is in a steady state, i.e., the change in C_{veg} over time (dC_{veg}/dt) equals zero, then vegetation carbon turnover times can be calculated as the ratio between vegetation carbon stock and GPP:

$$\tau_{SSA} = \frac{C_{veg}}{GPP} \quad (4)$$

Here SSA is calculated pixel-wise by using annual mean Cveg and GPP over the period of 1992-2016.

2.6 Estimation of under non-steady state

Compared with the estimations of under steady-state assumption, the changes in C_{veg} over time are considered (dC_{veg}/dt 0) when estimating under non-steady state ($_{NSSA}$). To derive a robust estimation of $_{NSSA}$ at each grid cell, we calculated $_{NSSA}$ using three different methods to assess the uncertainty built in the estimations.

2.6.1 Method 1

We estimate ΔC_{veg} by calculating the annual difference of C_{veg} between year t and year t – 1. Then, a estimate can be derived for each year by applying GPP and ΔC_{veg} at year t. Finally, we derive the under a non-steady state by averaging over time:

$$\tau_{\mathrm{NSSA}} = \frac{C_{veg,t-1}}{\mathrm{GPP}_t - C_{veg,t}} \quad (5)$$

2.6.2 Method 2

In the second method, we estimated the mean ΔC_{veg} using the trend of C_{veg} in a certain period to avoid the influence of outliers on the results. In this way, can be inferred as:

$$\tau_{\mathrm{NSSA}} = \frac{\overline{C_{\mathrm{veg}}}}{\overline{\mathrm{GPP}} - C_{veg,\ trend}} \quad (6)$$

Here the $C_{veg,\ trend}$ is inferred by applying a simple linear regression model (least-square robust fitting) between the response variable C_{veg} and time (C_{veg} ~ T). The coefficient of T is, therefore, the average annual ΔC_{veg} over the whole period. Thus, the under a non-steady state can be estimated with the annual mean values of C_{veg}, GPP, and ΔC_{veg}.

2.6.3 Method 3

In the third method, we infer from Eq.3 by applying a linear regression model (least-square robust fitting) at each grid cell in which (GPP - ΔC_{veg}) is the target variable while C_{veg} is the predictor, enabling annual turnover time to be inferred from the coefficient of C_{veg} ($1/\ _{\mathrm{NSSA}}$):

$$GPP - C_{\mathrm{veg}} \sim \frac{1}{\tau_{\mathrm{NSSA}}} \bullet C_{\mathrm{veg}} \quad (7)$$

Here ΔC_{veg} is the difference of C_{veg} between year t and year t - 1. GPP is the carbon input in year t and C_{veg} is the total carbon density in year t - 1, respectively.

3 Results

3.1 Comparison of under NSSA and SSA at grid cell level and global scale

The values (Figure 1) represent the turnover time of the entire forest living vegetation biomass, averaged over the whole period of the observations. The comparison between estimates of $_{\mathrm{NSSA}}$ using three different methods and $_{\mathrm{SSA}}$ shows a consistent pattern that carbon turnover processes are far from a steady state at the grid cell level (Figure 1, first row). Although there is a high correlation in the global spatial patterns (R2>0.98, bottom off-diagonal plots in Figure 1), differences between $_{\mathrm{NSSA}}$ and $_{\mathrm{SSA}}$ are characterized by high spatial heterogeneity. Although there are differences in the estimations of $_{\mathrm{NSSA}}$ that derived from the three methods, the

high global correlation and similar patterns of the difference between $_{NSSA}$ and $_{SSA}$ shows high consistency in the estimated $_{NSSA}$. Our results show a high spatial variability of values ranging from 0 to 15 years. The longest turnover times are located in the northern boreal forest ecosystem, where part of the biome has values longer than ten years, whereas carbon in the temperate forest ecosystem turnovers over much faster where the values are mostly under five years (Figure 2a). The assumption that vegetation biomass is in steady state results in an overall bias of by 10% (90^{th} percentile), compared to the estimates under a non-steady state at the grid cell level (Figure 1). This finding indicates that the majority of global forest ecosystems are not in a steady state, although the degree of deviation from a steady state differs from one region to another. The discrepancies between $_{SSA}$ and $_{NSSA}$ are substantially higher in the boreal forest (4.33%) ecosystem than in the tropical forest 10.99%) ecosystems indicating that the forests in the tropics are closer to a steady state, whereas assuming SSA in the boreal forest may cause large bias (Figure 2). Although the difference can be large at the grid cell level, there is a high global correlation ($r > 0.98$) between $_{SSA}$ and $_{NSSA}$ at the global scale, indicating an overall similar spatial pattern with or without considering the changes in annual biomass at the global scale. Here we show that the forest biomass at the global scale is roughly in a steady state whereas the SSA is largely violated at the grid cell level, especially in the northern boreal forest ecosystems where the values can be substantially underestimated or overestimated if assuming SSA.

In line with a previous study in which the SSA-induced biases are assessed at site level (Ge et al., 2019), we show that SSA causes significant underestimations of up to 40% (99th percentile) in China during the period of 2005-2015 (Figure S1). However, our results show a high heterogeneity where SSA can also cause overestimation of up to -12% (1th percentile). Further analysis shows that the pattern also changes across different periods of time. For instance, there is a contrasting pattern between 2001-2005 and 2009-2013 in which the former is characterized by overestimation of induced by SSA whereas there is a widespread underestimation of in the latter.

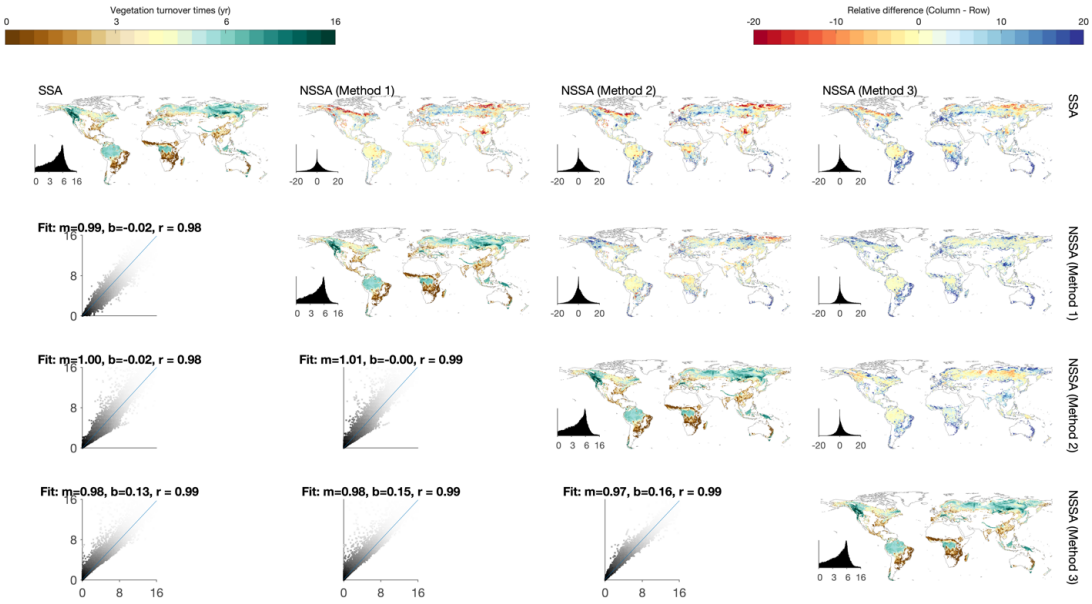

Figure 1. Comparison of under SSA and NSSA using different methods. The upper off-diagonal subplots show the relative difference between each pair of datasets (column/row). The bottom off-diagonal subplots show the density plots and major axis regression line between each pair of datasets (m: slope, b: intercept, r: correlation coefficient). The ranges of both of the color bars are between the 1st and the 99th percentiles of the data.

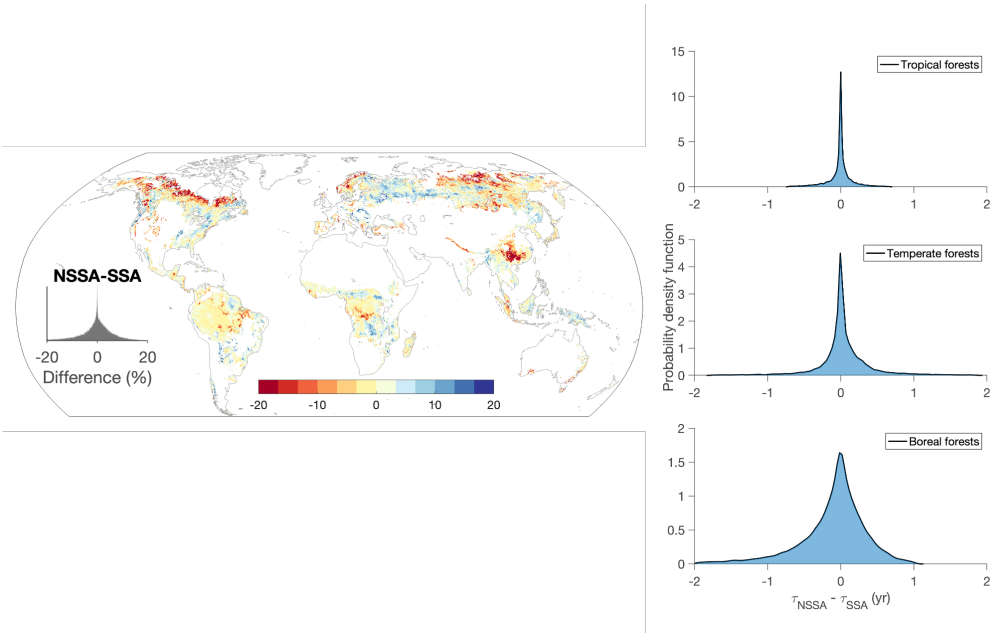

Figure 2. Spatial distribution of the relative difference (in percent) between $_{NSSA}$ and $_{SSA}$. The histograms show the probability distribution of $_{NSSA}$ - $_{SSA}$ (in years) in tropical forest, temperature forest and boreal forest. The $_{NSSA}$ shown here was estimated using Method 1.

3.2 The effect of large-scale disturbances on carbon turnover times

The disturbance from natural causes or anthropogenic activities can make an ecosystem deviate from a steady state. By estimating carbon turnover times at different periods, we quantified the degree of deviation if disturbances, e.g., deforestation, happened in a forest ecosystem. Figure 3 shows that the pervasive deforestation in the 90s primarily affected the carbon turnover times in the southeast part of the Amazon, which is known as the 'arc of deforestation' (hereafter AOD, Durieux et al., 2003). Our results clearly show $_{NSSA}$ is approximately 20% lower than $_{SSA}$ in the AOD region from 1993 to 1998, indicating anthropogenic activity (mostly deforestation) accelerated the carbon turnover rates to a large extent. Compared with the AOD, forests in the middle of Amazon, where there are less population and disturbances are closer to a steady state, as shown by the much less difference between $_{NSSA}$ and $_{SSA}$. Further analysis shows that tree canopy cover (Figure 3, Row 2) and C_{veg} (Figure 3, Row 3) changes decreased mainly during the same period of 1993-1998, whereas the changes in GPP does not follow the trend in the arc of deforestation. These results indicate that the acceleration

of turnover times during this period is directly caused by the large decrease in the vegetation biomass, which is intimately associated with a decrease in forest cover in this region. On the other hand, our findings show that the forest ecosystems started to recover during the 1999-2004 period as the vegetation biomass increased by 10% to 20%, in line with the increased tree canopy cover in the AOD region. As a result, the carbon turnover times increased by 10% to 30% during the same period. From 2011 to 2016, the magnitude of changes in , C_{veg} and tree canopy cover significantly decreased, indicating the forest ecosystems are closer to a steady state due to less disturbances. These findings indicate that turnover times and the steady state of the forest ecosystem can be largely affected by anthropogenic activities.

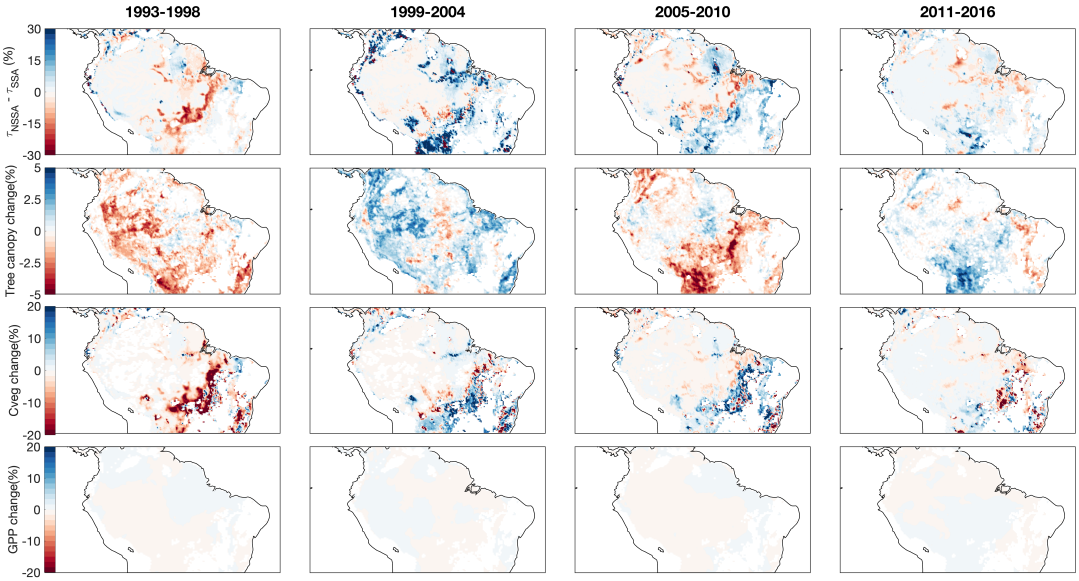

Figure 3. Regional changes in the relative difference between $_{NSSA}$ and $_{SSA}$ (($_{NSSA}$ - $_{SSA}$)/ $_{SSA}$*100) from 1993 to 2016, row 1, forest cover change (%), row 2, vegetation biomass change (%), row 3, GPP change (%), row 4 at different time periods in Amazon region.

3.3 The effect of spatial scale on the steady-state assumption

We further investigate the effect of spatial scale on the difference between $_{NSSA}$ and $_{SSA}$ in different biomes by gradually changing

the spatial scale from 0.25º (grid cell level) to 25º (continental scale). Here the difference between $_{\mathrm{NSSA}}$ and $_{\mathrm{SSA}}$ at each spatial scale is quantified by the 10, 50 and 90 percentiles of the relative difference between $_{\mathrm{NSSA}}$ and $_{\mathrm{SSA}}$ (Q_{10}, Q_{50}, Q_{90}, Figure 4). We find that the difference between $_{\mathrm{NSSA}}$ and $_{\mathrm{SSA}}$ substantially decreases with increasing spatial scales. The Q_{10} and Q_{90} tropical forests decrease by approximately 5%, whereas it decreases by approximately 10% in temperate and boreal biomes when the spatial scale increases from grid cell to ecosystem scale. Globally, the difference between $_{\mathrm{NSSA}}$ and $_{\mathrm{SSA}}$ is approximately 3% at ecosystem scale, indicating that steady state assumption will cause less errors in estimating carbon turnover times at larger spatial scales.

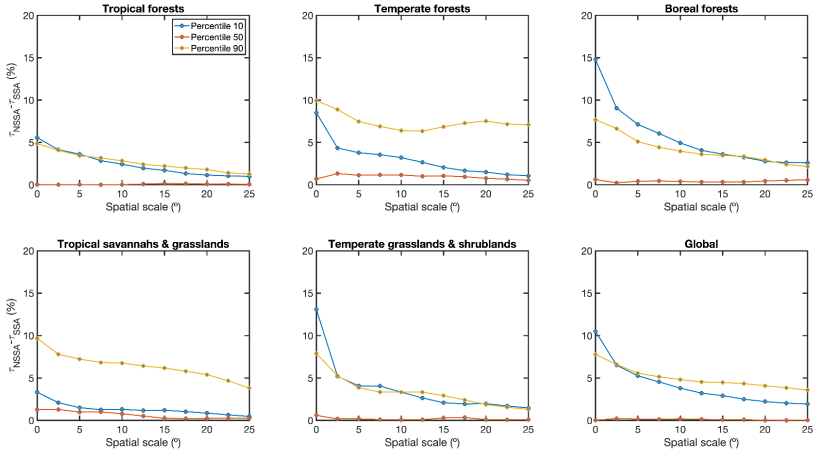

Figure 4. Effects of spatial scale on the difference between $_{\mathrm{SSA}}$ and $_{\mathrm{NSSA}}$. The x-axis represents the increase of spatial scales from grid cell level (0.25º) to continental level (25º). The y-axis represents the 10^{th} (absolute value) and 90^{th} relative difference between $_{\mathrm{NSSA}}$ and $_{\mathrm{SSA}}$.

4 Discussion

Our findings imply that the two different assumptions, i.e., SSA and NSSA, should be applied based on different ecological principles and spatial scales. The common approach of defining as the ratio between carbon stock and carbon influx based on SSA can be justified and properly applied when the changes in net carbon flux are negligible relative to the total carbon stock (Carvalhais et al., 2014). Although disturbances from nature or human beings could cause non-steady-state behavior, neglecting the changes, in some cases, only make a little difference to the quantification of the spatial pattern of , which does not hamper the understanding of the dynamics

of the terrestrial ecosystem carbon cycle. However, at a grid cell level, neglecting the changes in vegetation carbon (assuming vegetation is in a steady state) may result in a large bias. Using three methods, we provide robust estimations of under a non-steady state. The comparisons between $_{\mathrm{SSA}}$ and $_{\mathrm{NSSA}}$ show high heterogeneity in both space and time. A pioneer study (Ge et al., 2019) showed large SSA-induced biases on estimation in varied ecosystems of China by using the data at ten FLUXNET sites from 2005 to 2015 which is consistent with our results. However, we further show that the magnitude and the signs of the SSA-induced biases are characterized by high spatial heterogeneity and can change in time. This is mainly caused by the changes in vegetation biomass due to climate change or disturbances (Figure 3).

We have shown substantial heterogeneity in the degree of validity of the steady-state assumption across space. The comparison between $_{\mathrm{SSA}}$ and $_{\mathrm{NSSA}}$ quantitatively shows that most global forest ecosystems are far from steady-state, especially in the temperate and boreal forests. Even at regions of high biomass density such as Amazon Forest where the changes in vegetation carbon is relatively small, i.e., closer to steady-state, disturbances such as deforestation or fire could drive the forest ecosystem away from steady-state, as our results clearly show that the arc of deforestation in Amazon Forest have large difference between $_{\mathrm{SSA}}$ and $_{\mathrm{NSSA}}$ caused by drastic changes in vegetation biomass (Figure 3). These results indicate that applying SSA at the grid cell level is likely to cause substantial errors, potentially leading to misleading conclusions based on poor estimation of carbon turnover times.

Furthermore, our study quantified the link between spatial scales and the validity of SSA. Our results imply that SSA is approximately valid at large spatial scales (>15^{o} or 1500km), at which scale the differences are much lower (~5%) than grid cell level. The current understanding of the temporal dynamics of the terrestrial carbon cycle nearly all relies on earth system models in which the carbon turnover rates are retrieved under the SSA, which results in large discrepancies in carbon pools and turnover among different models (Friend et al., 2014; Todd-Brown et al., 2013). The estimation of under NSSA with observational long-term biomass data provides insights into better understanding and thus modeling turnover rate and its spatial patterns.

5 Conclusions

Our findings suggest that the steady state assumption is robust at a global scale yet becomes much less realistic at the grid cell level as the difference between regional $_{\mathrm{SSA}}$ and $_{\mathrm{NSSA}}$ can be as large as 20%. The usage of the steady state assumption would result in

a substantial bias of , especially in the region with a high degree of disturbance, either from human beings or natural causes. However, at a larger spatial scale, the differences in estimations at SSA and NSSA significantly decrease because the annual changes in vegetation biomass are small compared with the total amount of biomass. With the novel long-term observations of vegetation biomass, we revealed a detailed picture of the spatial distribution of carbon turnover times under different assumptions and its relationship with spatial scales, which will guide the proper application of the two assumptions on different conditions.

Acknowledgments

N.F. acknowledges support from the International Max Planck Research School for Biogeochemical Cycles (IMPRS-gBGC). S.K. acknowledges support from the CRESCENDO project of the European Union's Horizon 2020 Framework Programme (grant agreement no. 641816).

Author Contributions

N.F. and N.C. designed the analysis of this research and wrote the manuscript with contributions from all authors.

References

Besnard, S., Santoro, M., Cartus, O., Fan, N., Linscheid, N., Nair, R., et al. (2021). Global sensitivities of forest carbon changes to environmental conditions. *Global Change Biology*, *27*(24), 6467–6483. https://doi.org/10.1111/gcb.15877Carvalhais, N., Forkel, M., Khomik, M., Bellarby, J., Jung, M., Migliavacca, M., et al. (2014). Global covariation of carbon turnover times with climate in terrestrial ecosystems. *Nature*, *514*(7521), 213–217. https://doi.org/10.1038/nature13731Durieux, L., Machado, L. A. T., & Laurent, H. (2003). The impact of deforestation on cloud cover over the Amazon arc of deforestation. *Remote Sensing of Environment*, *86*(1), 132–140. https://doi.org/10.1016/S0034-4257(03)00095-6Eggleston, H. S., Buendia, L., Miwa, K., Ngara, T., & Tanabe, K. (2006a). 2006 IPCC Guidelines for National Greenhouse Gas Inventories. Retrieved from https://www.osti.gov/etdeweb/biblio/20880391Eggleston, H. S., Buendia, L., Miwa, K., Ngara, T., & Tanabe, K. (2006b). 2006 IPCC guidelines for national greenhouse gas inventories.Friedlingstein, P., Cox, P., Betts, R., Bopp, L., Bloh, W. von, Brovkin, V., et al. (2006). Climate–Carbon Cycle Feedback Analysis: Results from the C4MIP Model Intercomparison. *Journal of Climate*, *19*(14), 3337–3353. https://doi.org/10.1175/JCLI3800.1Friend, A. D., Lucht, W., Rademacher, T. T., Keribin, R., Betts, R., Cadule, P., et al. (2014). Carbon residence time dominates uncertainty in terrestrial vegetation responses to future climate and atmospheric CO2. *Proceedings of the National Academy of Sciences*, *111*(9), 3280–3285. https://doi.org/10.1073/pnas.1222477110Ge,

R., He, H., Ren, X., Zhang, L., Yu, G., Smallman, T. L., et al. (2019). Underestimated ecosystem carbon turnover time and sequestration under the steady state assumption: A perspective from long-term data assimilation. *Global Change Biology*, *25*(3), 938–953. https://doi.org/10.1111/gcb.14547Huang, Y., Ciais, P., Santoro, M., Makowski, D., Chave, J., Schepaschenko, D., et al. (2021). A global map of root biomass across the world's forests. *Earth System Science Data*, *13*(9), 4263–4274. https://doi.org/10.5194/essd-13-4263-2021Jung, M., Schwalm, C., Migliavacca, M., Walther, S., Camps-Valls, G., Koirala, S., et al. (2020). Scaling carbon fluxes from eddy covariance sites to globe: synthesis and evaluation of the FLUXCOM approach. *Biogeosciences*, *17*(5), 1343–1365. https://doi.org/10.5194/bg-17-1343-2020Santoro, M., Beer, C., Cartus, O., Schmullius, C., Shvidenko, A., McCallum, I., et al. (2011). Retrieval of growing stock volume in boreal forest using hyper-temporal series of Envisat ASAR ScanSAR backscatter measurements. *Remote Sensing of Environment*, *115*(2), 490–507.Santoro, M., Cartus, O., Wegmüller, U., Besnard, S., Carvalhais, N., Araza, A., et al. (2022). Global estimation of above-ground biomass from spaceborne C-band scatterometer observations aided by LiDAR metrics of vegetation structure. *Remote Sensing of Environment*, *279*, 113114. https://doi.org/10.1016/j.rse.2022.113114Song, X.-P., Hansen, M. C., Stehman, S. V., Potapov, P. V., Tyukavina, A., Vermote, E. F., & Townshend, J. R. (2018). Global land change from 1982 to 2016. *Nature*, *560*(7720), 639–643. https://doi.org/10.1038/s41586-018-0411-9Thurner, M., Beer, C., Carvalhais, N., Forkel, M., Santoro, M., Tum, M., & Schmullius, C. (2016). Large-scale variation in boreal and temperate forest carbon turnover rate related to climate. *Geophysical Research Letters*, *43*(9), 4576–4585. https://doi.org/10.1002/2016GL068794Todd-Brown, K. E., Randerson, J. T., Post, W. M., Hoffman, F. M., Tarnocai, C., Schuur, E. A., & Allison, S. D. (2013). Causes of variation in soil carbon simulations from CMIP5 Earth system models and comparison with observations. *Biogeosciences*, *10*(3).Tramontana, G., Jung, M., Schwalm, C. R., Ichii, K., Camps-Valls, G., Ráduly, B., et al. (2016). Predicting carbon dioxide and energy fluxes across global FLUXNET sites with regression algorithms. *Biogeosciences*, *13*(14), 4291–4313. https://doi.org/10.5194/bg-13-4291-2016